Chinese Chemical Letters 33 (2022) 4924–4929

Contents lists available at ScienceDirect

Chinese Chemical Letters

journal homepage: www.elsevier.com/locate/cclet

Oral colon-targeted mucoadhesive micelles with enzyme-responsive controlled release of curcumin for ulcerative colitis therapy

Chen Zhang[a,1], Jiaxin Li[a,1], Meng Xiao[a], Di Wang[a], Yan Qu[a], Liang Zou[b], Chuan Zheng[a,c,*], Jinming Zhang[a,*]

[a] State Key Laboratory of Southwestern Chinese Medicine Resources, School of Pharmacy, Chengdu University of Traditional Chinese Medicine, Chengdu 611130, China
[b] Key Laboratory of Coarse Cereal Processing, Ministry of Agriculture and Rural Affairs, Chengdu University, Chengdu 610106, China
[c] Oncology Teaching and Research Department, Hospital of Chengdu University of Traditional of Chinese Medicine, Chengdu 610072, China

ARTICLE INFO

Article history:
Received 9 December 2021
Revised 29 March 2022
Accepted 29 March 2022
Available online 2 April 2022

Keywords:
Curcumin
Enzyme-responsive
Micelles
Mucoadhesion
Ulcerative colitis

ABSTRACT

Although multitudinous nanoscale drug-delivery systems (DDSs) have been recommended to improve anti-ulcerative colitis (UC) outcomes, to enhance the mucoadhesion of nanosystems on the colon and specifically release the loaded drugs in response to the colon micro-environment would be critical factors. The application of curcumin (Cur), an acknowledged anti-UC phytochemical compound, for UC therapy requires more efficient nano-carriers to improve its therapeutic outcome. Herein, we developed the colon-targeted nano-micelles with mucoadhesive effect and Azo reductase-triggered drug release profiles for Cur delivery in UC treatment. Specifically, the amphiphilic block polymer containing the Azo-reductase sensitive linkage (PEG-Azo-PLGA), and catechol-modified TPGS (Cat-TPGS) were synthesized respectively. Based on the self-assembly of the mixed polymers, Cur-micelles (142.7 ± 1.7 nm of average size, 72.36% ± 1.54% of DEE) were obtained. Interestingly, the Cur-micelles exhibited the Azo-reductase sensitive particle dissociation and drug release, the enhanced cellular uptake and the prolonged retention on colonic mucosa, mediated by the strong mucoadhesion of catechol structure. Ultimately, Cur-micelles significantly mitigated colitis symptoms and accelerated colitis repair in DSS-treated mice by regulating the intestinal flora and the levels of pro-inflammatory factors (MPO, IL-6, IL-1β, and TNF-α) related to TLR4/MyD88/NF-κB signaling pathway. This work provides an effective drug delivery strategy for anti-UC drugs by oral administration.

Ulcerative colitis (UC) is a common inflammatory disease in the colon, which is characterized by diarrhea, mucosal ulceration, and rectal bleeding. In recent years, this disease affects several million patients worldwide, the incidence of UC is rapidly increasing worldwide, especially in many developing countries [1]. Although a lot of efforts have been made to find the reasons for the genesis and development of UC, its etiology still remains unclear to date. Currently, the therapeutics for UC mainly relies on the utilization of anti-inflammatory agents, immunomodulatory drugs and biological products. Several medications used in clinic to alleviate the symptoms of UC, such as corticosteroids, amino-salicylates and infliximab, confront the poor therapeutic efficiency as well as the frequent side-effects. Curcumin (Cur), a natural anti-inflammatory polyphenol compound derived from *Curcuma longa* L., has been well-acknowledged demonstrated to ameliorate UC in several previous studies [2,3]. Most importantly, Cur also possess the high safety as a "generally regarded as safe" compound by FDA [4,5]. Collectively, these results suggest that Cur could act as a promising therapeutic agent for UC therapy.

Nevertheless, impacted by the potential structural failure in gastrointestinal tract [6,7], Cur commonly requires the vehicle encapsulation to carry out the specific colon-targeting delivery. Nanoscale drug delivery systems, promising for improving the pharmacokinetics, bioavailability and solubility exhibited by drug [8–12] (*e.g.*, liposomes, micelles and nano-gels), are demonstrated with bright prospect for UC therapy. Moreover, for the improvement of drugs' influence for treating ulcerative colitis, the nanoscale drug delivery system should exhibit the two characteristics of long-term retention of colon tissue and controlled release of the colon. One good candidate is catechol group with high presence within sticky marine mussel foot protein and contributes to

* Corresponding authors.
E-mail addresses: zhengchuan@cdutcm.edu.cn (C. Zheng), cdutcmzjm@126.com (J. Zhang).
[1] These authors contributed equally to this work.

https://doi.org/10.1016/j.cclet.2022.03.110
1001-8417/

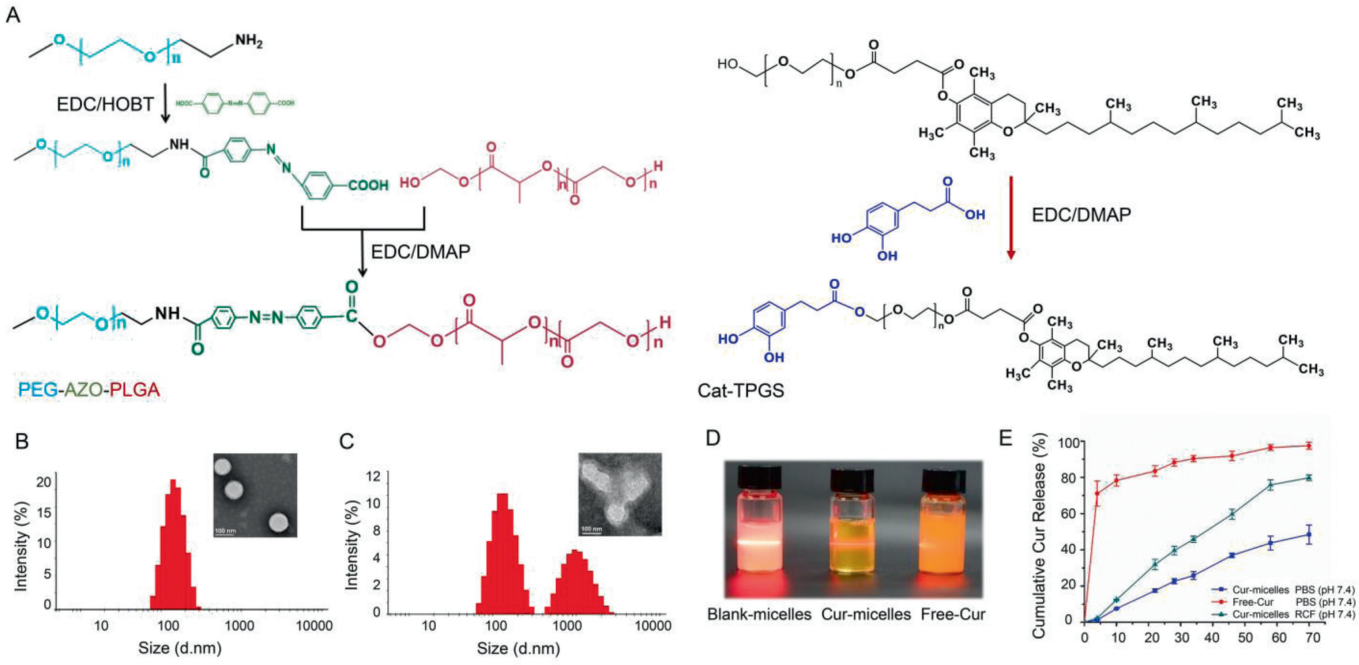

Fig. 1. Physical and chemical characterization of Cur-micelles. (A) The total synthesis routes of PEG-Azo-PLGA and Cat-TPGS. (B) The particles size distribution by DLS and the TEM images of the Cur-micelles. Scale bar: 100 nm. (C) The particle size distribution and TEM images of Cur-micelles in rat colon fluid. Scale bar: 100 nm. (D) The photograph: Control NPs, Cur-micelles, Free-Cur. (E) Cumulative release present of Cur from the Cur-micelles in different medium at 37 °C.

the significant mussel' underwater adhesion onto various surfaces [13]. Catechol is available for enhancing polymeric materials' mucoadhesion through the formation of bonds that are covalent and not covalent with mucin. Several existing studies investigated the mucoadhesive properties of catechol. For instance, on the basis of catechol end-functionalization, PEG, short for poly (ethylene glycol), a non-mucoadhesive polymer, was converted into a mucoadhesive polymer [14]. Jinke Xu *et al.* developed mucoadhesive hydrogel for facilitating rectal sulfasalazine administration in treating UC [15]. A number of approaches in terms of drug delivery specific to colon were developed, covering methods exploiting pressures, times, pH values and/or bacteria [16–18]. Colonic microflora covers anaerobic bacterium merely existing within the region of colon and secretes particular biodegradable enzyme, thereby facilitating colonic drug release targeting [19,20]. The Azo bond in polymer is available to be a bacteria-triggered colon-targeted sensitive bond.

The design and evaluation of a multiple functional polymeric micellar system loading Cur (Cur/micelles) for UC therapy were reported here to facilitate the prolonged colon retention and colon specific enzyme-responsive release of Cur (Graphical abstract). First, the synthesis an Azo-linked PEG-PLGA polymer was achieved under graft modification reactions (Fig. 1A). The chemical structures of PEG-Azo-PLGA were obtained (Fig. S1A in Supporting information). The 8.31 ppm (e), 8.25 ppm (f), 8.11 ppm (c) and 8.03 ppm (d) were the characteristic ^{1}H NMR spectra on the benzene ring of Azo. The typical peaks 5.23 ppm, 4.89 ppm and 1.55 ppm of PLGA appeared, as represented by j, i and h. The typical peaks 3.59 ppm and 4.83 ppm were labeled b and a belonged to –CH_2-CH_2-O of the mPEG. Therefore, based on the ^{1}H NMR spectra results, the introduction of Azo bond was successful.

Subsequently, 3,4-dihydrohydrocinnamic acid was modified on the PEG1000 moiety of TPGS to obtain the catechol modified TPGS (Cat-TPGS) (Fig. 1A). The Cat-TPGS (Fig. S1B in Supporting information) were confirmed on the basis of ^{1}H NMR. The peaks 3.56 ppm (f), 2.70-1.95 ppm (g), 1.60-1.11 ppm (h) and 0.89 ppm (i) belonged to the characteristic ^{1}H NMR spectra of the TPGS. 0.89 ppm (i) and 3.56 ppm (f) signals indicated the feature exhibited by -CH_3 as well as O-CH_2-CH_2 protons of TPGS side chain's long-chain alkyl group. The typical peaks 9.57 ppm, 8.84 ppm, 6.89 ppm, 6.71 ppm and 6.55 ppm of Cat appeared at which were labeled a, b, c, d and e. On the whole, the mentioned result demonstrated the effective synthesis.

The collected Cur loaded in PEG-Azo-PLGA/Cat-TPGS polymers (Cur-micelles) had almost 142.7 nm mean diameter exhibiting a narrow distributing characteristic (Table S1 in Supporting information). Cur loading's drug entrapment efficiency (DEE) as well as drug loading efficiency (DLE) within NPs reached 72.36% ± 1.54% as well as 4.21% ± 0.56%, respectively. Fig. 1B illustrates how the morphology is distributed on the basis of transmission electron microscopy (TEM) observation, as well as how the size of Cur-micelles is distributed on the basis of dynamic light scattering (DLS). The Cur-micelles were characterized by firmly packed structure, regular spherical form, and a uniform size distribution. Nevertheless, for responding rat colon fluid medium in terms of the mimicking of the colonic flora small habitat distinctly specialized and effectively isolated, the size distributions of Cur-micelles started to be elevated according to several peaks. Cur-micelles were characterized by the fragmented and dispersed uniform orbicular morphology (Fig. 1C). Furthermore, compared with the Free-Cur suspension liquid, the Tyndall phenomenon formed by the laser beam transmitted through the nano-solution was significant (Fig. 1D).

For the verification of the colon-targeted drug delivery's targeting specific to colon as well as azo enzyme-responsive cleavage, this study compared the Cur release from micelles in different experimental conditions (Fig. 1E). Compared with that in PBS, Cur cumulative release from sensitive polymer nanoparticles was noticeably expedited within the colonic fluid of the rat. At the end of 72 h release, the Cur release from polymer micelles in rat colonic fluid was 76.5% of initial load of Cur. However, the cumulative Cur under the release by sensitive polymer nanoparticles in PBS was nearly 42.3%. Besides, because Cur was not nano-crystallized, Free-Cur was released in PBS quickly, and 71% of the total Cur can be released in 4 h. According to the mentioned result, the polymers' azo bond critically impacts Cur originating from Cur-loaded poly-

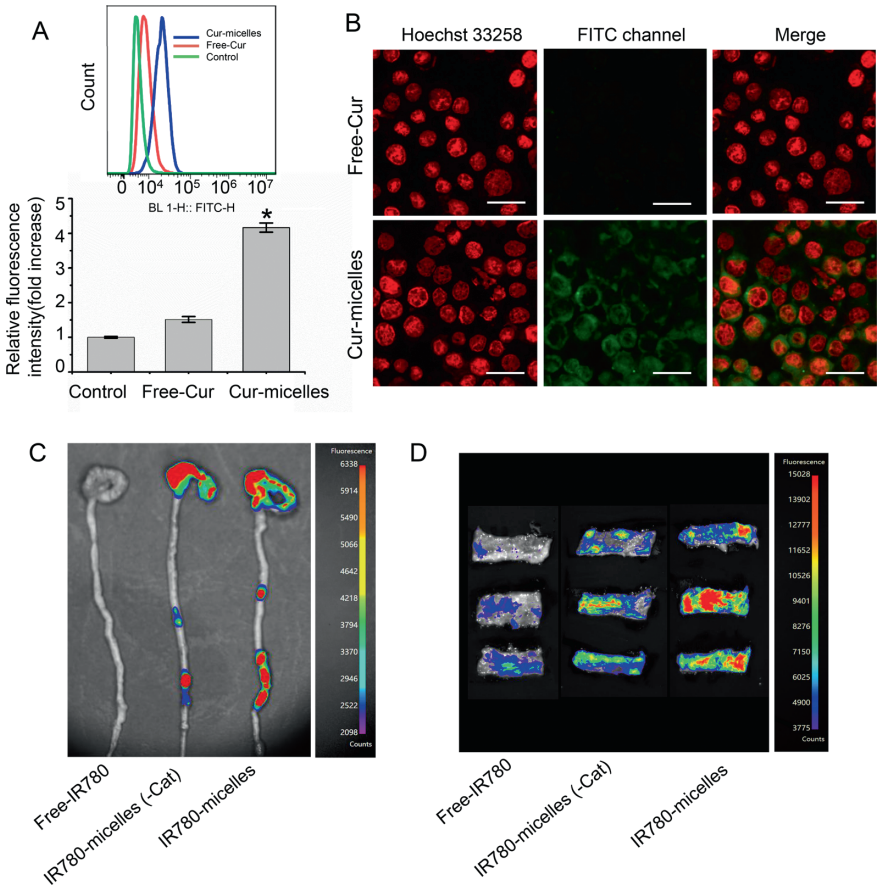

Fig. 2. (A) Quantitative measure of Cur uptake in different Cur formulations (Free-Cur and Cur-micelles) after incubation for 4 h. Cur incubation concentration was 16 μg/mL. (B) Fluorescent images of Caco-2 cells incubated with different Cur formulations (Free-Cur and Cur-micelles) for 4 h; scale bar: 100 μm. Cur incubation concentration was 16 μg/mL ($^{*}P < 0.05$ *vs.* Free-Cur). (C) *In vivo* colon targeting and retention of Cur-micelles in colitis mice, the colon tissues in each cohort were dissected and observed by *ex vivo* fluorescence imaging (24 h post-administration). (D) *Ex vivo* fluorescence images of rat colons after incubation at 37 °C across different formulation.

mer micelle, thereby causing greater Cur content within the part of colon and satisfying drug delivery's requirement with the target of colon.

Cur-micelle uptake manner was measured with the use of flow cytometer (FCM). Confocal laser scanning microscopy (CLSM) was used to observe cells. The FCM profile and histogram Cur average intensity was elevated over time or according to the dosage of Cur (Figs. S2A and B in Supporting information), thereby demonstrating the cell-uptake efficacy in Cur-micelle's Caco-2 cells on a basis relying on time or relying on dosage, separately. According to the cell-uptake ability, nanoscale is capable of enhancing Cur-micelle's cell-uptake efficacy on a basis relying on time or relying on dosage, primarily accounting for Cur-micelle's prominent efficacy, other than Free-Cur. High efficiency intracellular uptake refers to a main requirement in terms of using Cur for treatment purposes. According to Fig. 2A, as Caco-2 cell was incubated by using various Cur formulations (Cur-micelles as well as Free-Cur) under the period of 4 h, Cur intensity within Cur-micelle exceededFree-Cur's, according to the mean fluorescence intensity's histogram results and FCM-detection profiles. Thus, fluorescence microscopy result was demonstrated (Fig. 2B), and Cur-micelle's significant cell-uptake ability was proven. In addition, the system's great uptake capacity is likely to be because of the nanoscale of the system. We used confocal microscope for confirming the cellular uptake profiles regarding Caco-2 cells' Cur-micelles as well asFree-Cur at the incubation time point of 4 h (Fig. 2B). As expected, this study measured the clear Cur accumulation from cells under the Cur-micelle treatment. Cur fluorescence signals within the cells under the Cur-micelle treatment outperformed cells under theFree-Cur treatment. According to the mentioned result, Cur-micelle could achieve the delivery of a greater amount of Cur within Caco-2 cell as compared with Free-Cur.

For the mentioned reason, micelles' the colitis targeting capability *in vivo* and retention capability were proved. IR780, an NIR dye exhibiting a maximal absorbance at 780 nm, was sealed within PEG-Azo-PLGA/Cat-TPGS micelles or PEG-Azo-PLGA/TPGS micelles (termed IR780-micelles and IR780-micelle(-Cat)). Colitis mice took nanoparticle's solution orally. With the use of IVIS spectrum under a range of times after intragastric administration, we captured NIR fluorescence image. According to Fig. S3 (Supporting information), the IR780-micelles Group's mean fluorescence intensity was significantly greater as compared with that of Free-IR780 and IR780-micelles(-Cat) at 6, 12, and 24 h after intragastric administration. At 6 h after intragastric administration, the Cat-IR780-micelles group's mean fluorescence intensity *in vivo* reached three times that of Free-IR780. At 24 h after intragastric administration, the mean fluorescence intensity was reduced noticeably within colitis rats. Nevertheless, Cat-IR780-micelles group's mean fluorescence intensity was continuously greater as compared with that of other groups. The colons were collected after the sacrifice of rats at 24 h post intragastric administration. According to Fig. 2C, the mean fluorescence intensity exhibited by IR780-micelles group' colon was obviously higher than other group.

For the observation of IR780-micelle's adhesion ability to inflame mucosa, we took the colon with inflammation from the UC rat model with the use of TNBS administration. Next, we captured

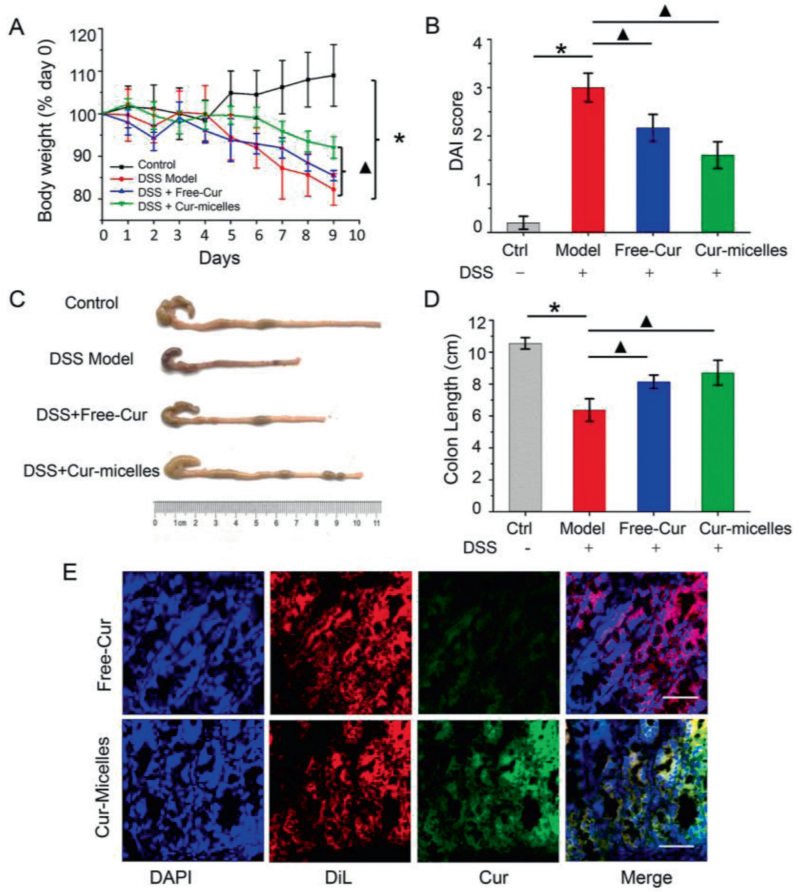

Fig. 3. (A) The daily weight change in different group of mice. (B) DAI scores of mice in various groups. (C) Representative photographs of mice's colons in various groups. (D) Colon length of mice in various groups. (E) Frozen section of colitis tissues after drug administration. Red, DiL (cell membrane); Blue, DAPI (nucleus); Green, Cur. $^{*}P < 0.05$ untreated control group *vs.* DSS-induced UC model group, $^{▲}P < 0.05$ model group *vs.* treatment groups ($n = 6$ per group).

the images of Colon tissues *ex vivo* with the use of living imaging system for the comparison of IR780's fluorescence intensity under the attachment onto the colon tissue mucosa. According to Fig. 2D, after rinsed with PBS buffer solution, Free-IR780 fluorescence intensity decreased rapidly while the fluorescence intensity exhibited by IR780-micelles noticeably exceeded that of IR780-micelles(-Cat) or Free-IR780.

According to this animal experiment, we adopted a method to prevent DSS-induced UC after administration to assess the Cur-related nano-formulations for the prevention and treatment of colitis. The administration time of Cur was 9 days, and the time of DSS-induced colitis in mice was 7 days. Rats' body weight changes in the overall process of the experiment noticeably revealed the physiological state. According to Fig. 3A, a significant body weight loss of DSS-treated UC mice at day 9, as compared with the control. However, mice in Cur-micelles group exhibited a less distinct weight loss compared with model group. Given the mentioned typical clinical characteristics, we employed the DAI for the assessment of Cur therapeutic activity. All experiment on animals were carried out with a protocol approval from Chengdu University of TCM's the Animal Welfare Committee. The researchers' animal experimental processes based on the experimentally related protocol in accordance with the Guidelines for the Care and Use of laboratory Animal of the Ministry of Science and Technology of China. According to Fig. 3B, DAI scores of rats under the treatment by using DSS were noticeably grew as opposed to the control's. Nevertheless, Cur-micelles group's DAI scores noticeably declined, thereby demonstrating Cur-micelles' improvement on UC-associated pathological state. Besides the severe edema, hyperemia as well as synechia, the colon length of rats under the treatment by using DSS significantly declined. According to Figs. 3C and D, mouse' colon shortening under the treatment by using DSS. Thus, Cur-micelles administration was capable of noticeably ameliorating the shortening of the colon. According to Fig. 3E, few of Cur could be identified in submucosa of the colon after mice administrated by Free-Cur. However, the green fluorescence intensity in Cur-micelles treatment group noticeably exceeded the Free-Cur groups', thereby demonstrating that Cur-micelles could effectively accumulate and penetrate in colitis tissue after oral administration. The mentioned results indicate catechol chemical modification TPGS exhibits a great capability to be adherent to colon mucosa.

Within the immunization system of intestinal mucosa, neutrophil and macrophage contribute to the secretion of inflammation cytokine, thereby disrupting epithelial integrity and causing colon injury [21]. Neutrophils activated largely carried out the secretion of MPO. The MPO generally indicates inflammation severity [22]. According to Fig. S5 (Supporting information), within the DSS model group, colonic MPO activities showed significant elevation in comparison with the healthy control's. As compared with the other DSS groups, the group under the treatment of Cur-micelle exhibited the minimal colonic MPO activity. For this reason, intestinal injury characteristic within IBD and inflammatory response critically impact UC pathogenesis. Pro-inflammatory

cytokine production rose noticeably within model group under the induction of DSS in comparison with the control. Nevertheless, Cur-micelles administration down-regulated the not normally risen pro-inflammatory cytokine amounts (Fig. S5). The risen amounts of IL-1β, IL-6 and TNF-α showed correlation to the superficial ulcer as well as inflamed mucosa within UC mice. Accordingly, Cur-micelles noticeably eliminated the mentioned risen pro-inflammatory cytokines, which exhibited the highest efficacy.

Toll-like receptors (TLRs) are membrane-anchored proteins that are expressed on immune cells and enterocytes. TLRs act as pathogen recognition receptors (PRP), identifying microbe-associated molecular patterns (MAMPs) to activate specific signaling pathways [23]. Thirteen members of the TLR family have been confirmed in mammals, of which, TLR4 has been the most widely studied [24]. Several studies have suggested that TLR4 serves as the main mediator of responses to lipopolysaccharide (LPS) both *in vitro* and *in vivo*, and TLR4 signaling promotes intestinal damage in DSS-induced colitis [25]. The unbalanced microbiota can elicit intestinal not only through its LPS binding to intestinal toll-like receptor 4 (TLR4) but also through inducing elevation of LPS by altering gut microbiota composition [26]. According to new evidences, the inflammation response of UC receives a major regulation from TLR4/MyD88/NF-κB pathway [27]. Due to a risen intestinal permeability within UC cases, pathogenic microorganisms and toxic substances could cross the intestinal wall, thereby activating TLR4 [28]. TLR4 activation could activate MyD88, a vital adaptor molecule vital to TLR signaling, thereby activating downstream NF-κB signaling pathway and synthesizing pro-inflammatory cytokines (*e.g.*, IL-6, IL-1β and TNF-α facilitating UC growth) [29]. Besides, NF-κB is critical to interaction of gut microbiota, as well as mucosal immune system epithelial barrier function disruption [30]. Under the NF-κB activation triggered by DSS was related to TLR4. This study attempted to assess classical proteins by Western blotting investigation for exploring Cur's effect in this channel, and further study Cur-micelles (Fig. S4A in Supporting information). According to Fig. S4A, in comparison with the control, the total protein expression of TLR4, MyD88 and NF-κB p65 in colon tissue of Model group was evidently enhanced ($^{*}P < 0.05$). It is noteworthy that the mentioned three proteins' expressions within Cur-micelles group were noticeably less than others' ($^{\blacktriangle}P < 0.05$). In brief, Free-Cur and Cur-micelles are capable of inhibiting TLR4/NF-κB signaling pathway commendably.

Given the findings above, DSS could induce severe inflammation of colon tissues. The histopathological screening of mice' colon section by HE-staining revealed no necrosis or inflammation in the control (Fig. S4B in Supporting information). Mice in the DSS model group showed colon tissue injuries, including crypt distortion, goblet cell loss, severe epithelia damage, and mucosal inflammatory cell infiltration. Nevertheless, Cur-micelle administration was capable of noticeably protecting colon crypt structures and reducing histologic inflammations. Besides, the hypothesis was that Cur could protect the intestinal mucosa from damages by reinforcing its self-repair. To further demonstrate this hypothesis, periodic acid Schiff hematoxylin (PAS) staining was conducted for exploring the intestinal mucosa variation post Cur administration in the course of the DSS treatment. According to Fig. S4B, DSS + Oral-Cur-micelles treated mice colons possessed significant proportion of regenerative colonic crypts with mucus producing goblet cells morphology, closer to the healthy colon as compared with the colon from mice under colitis. For further confirming Cur-micelles' toxicity, we carried out the investigation of internal organs as well as H&E staining. According to Fig. S6 (Supporting information), after treatment, the harvested major organs (heart, liver, spleen, lung and kidney) from all mice showed no histopathological evidence of damage. The mentioned findings indicate the prominent Cur-micelle's biocompatibility and low toxicity.

Gut microbiota, a vital intestinal barrier component, significantly impacts host physiological process regarding the energy metabolism, nutrient absorption and immune system growth, as well as intestinal mucosal barrier function's maturation [31]. Cut microbiota dysfunction could cause the increased permeability of the intestinal epithelial cell, trigger mucosal inflammatory response, and promote the development of colitis. For this reason, regulation of intestinal microbiota is recognized to be a therapeutic approach in terms of UC patients. Cur was found to regulate gut microbiota structure and reduce its diversity in UC mice and therefore relieve the symptoms of UC [4]. In the present study, the expression of 16S rRNA gene sequence was employed to assess the amelioration of Cur-micelles on DSS-induced UC. The rarefaction curve plateau (Fig. S7A in Supporting information) with the current sequencing indicates that most of the diversities have already been captured in all samples. According to (Fig. S7B in Supporting information), we suggested microbial communities' alpha diversity with the use of Simpson index. Furthermore, the alpha diversity declined noticeably under the influence of DSS treatment, and microbial diversity remarkably increased under Cur-micelle administration. Under the weight Unifrac distance matrixes, according to the analyses of PCA (Fig. S7C in Supporting information) and PCoA (Fig. S7D in Supporting information), three groups' gut microbiota had noticeable diversification. Though Free-Cur and Cur-micelle administration failed to overall reverse the gut microbiota to the control's, Free-Cur or Cur-micelles could maintain the capability to regulate not normal gut microbiota within DSS-induced UC rats.

We employed histograms for indicating the difference in all groups in terms of intestinal microbiota's species and relative abundance. On the basis of the phyla level (Fig. 4A), *Proteobacteria*, *Firmicutes* and *Bacteroidetes* were reported as the predominant and most numerous species in all groups. Compared with the control, the intestinal microbial abundance of DSS-induced colitis mice noticeably grew within *Proteobacteria* and remarkably declined within *Firmicutes*. Inflammatory bowel disease was characterized by the significantly reduced *Firmicutes* [32]. And, the *Proteobacteria* are generally regarded as "microbial markers" of intestinal microbial disorders [33]. After Cur treatment, the variations in the intestinal flora of mice in the Free-Cur group and the Cur-micelles group were consistent with those in the control, which indicated an increase in *Firmicutes* and a decrease in *Proteobacteria*. As demonstrated by this result, Cur could inhibit the expansion of *Proteobacteria* in the colon of mice induced by DSS, which may show potential benefits for maintain intestinal homeostasis.

At the family level (Fig. 4B), according to the intestinal flora structure of DSS-induced UC mice compared with the control, the abundance of *Lachnospiraceae* and *Ruminococcaceae* declined, and *Bacteroidaceae* and *Burkholderiaceae* had increasing abundance. To be specific, *Lachnospiraceae* and *Ruminococcaceae* pertain to *Firmicutes*, which can promote the production of butyric acid in short-chain fatty acids in the intestine [34], while *Bacteroidaceae* is correlated with intestinal inflammation [35]. In comparison with the model group, after oral treatment with Free-Cur and Cur-micelles, the mouse flora structure rose in the abundance of *Lachnospiraceae* and *Ruminococcaceae*, while the abundance of *Bacteroidaceae* declined.

At the genus levels (Fig. 4C), compared with the control, DSS-induced colitis mice showed a significant decrease in the abundance of *Prevotellaceae UCG-001*, and a significant increase in *Helicobacter* and *Escherichia-Shigellaming*. To be specific, *Bacteroidetes/Prevotellaceae UCG-001* is correlated with the synthesis of SCFAs, and the secretion of SCFAs may help protect the intestinal mucosal barrier [36]. *Helicobacter* rises the severity of DSS-induced colitis [37]. *Enterobacter-Shigella* refers to typical pathogenic bacteria, which may help the destruct the tight junctions of the mucosal barrier and elevate the risk of bleeding from intestinal ulcers. Nev-

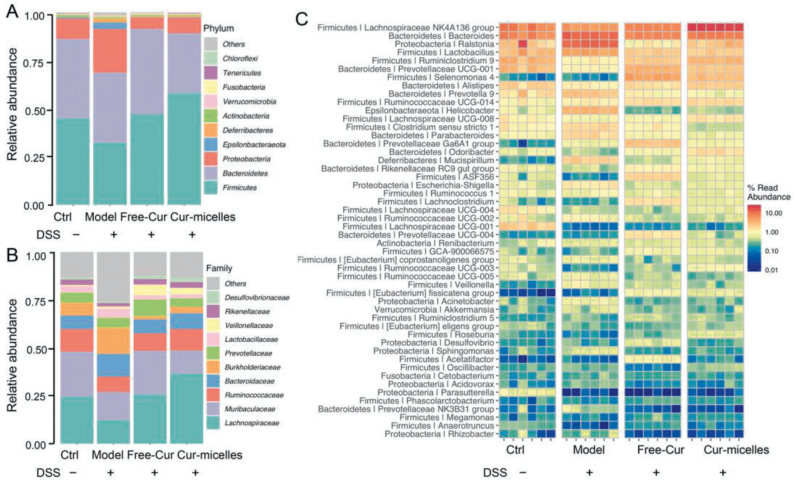

Fig. 4. Gut microbial community structure of mouse from various groups. (A) Community abundance analysis at phylum level. (B) Community abundance analysis at family level. (C) Community heat map of different groups at genus level. The color of the spot corresponds to the normalized and log-transformed relative abundance of genus.

ertheless, after oral treatment with Free-Cur and Cur-micelles, the abundance of the above three types of intestinal bacteria all tended to the level of the normal group. As confirmed by the result above, oral administration of Cur or Cur-micelles is capable of regulating the intestinal flora of mice and reducing the structural destruction of the intestinal flora of mice induced by DSS.

In brief, we successfully synthesized an amphiphilic block polymer PEG-Azo-PLGA and catechol structure modified TPGS, and self-assembled Cur-micelles with the use of the solvent evaporation method. According to the enzyme sensitivity test results, the Cur-micelles could be destroyed by the azoreductase within the rat colon solution and exhibit high enzyme sensitivity. As indicated by *in vivo* anti-UC test results, Cur-micelles could inhibit DSS-induced inflammation of the colon by regulating the TLR-4/MyD88/NF-κB signaling pathway, while helping regulate intestinal flora. On the whole, we reported a novel strategy, which can be very efficient in delivering Cur to colon based on enzyme-responsive and mucoadhesive polymer mixed micelles, so it can act as a potential method for curing UC.

Declaration of competing interest

The authors declare that they have no known competing financial interests or personal relationships that could have appeared to influence the work reported in this paper.

Acknowledgments

This work was supported by the National Natural Science Foundation of China (No. 81903811), China Postdoctoral Science Foundation (No. 2021M690488) and National TCM Multidisciplinary Interdisciplinary Innovation Team Project: Multidisciplinary Evaluation of Southwest Characteristic TCM Resources Multidisciplinary Interdisciplinary Innovation Team (No. ZYYCXTD-D-202209). Besides, we express our great appreciation to Jiayi Sun at Innovative Institution of Chinese Medicine and Pharmacy, Chengdu University of Traditional Chinese Medicine, for the assistance with confocal laser scanning microscopy. And, the authors wound like to thank Ting Du from Shiyanjia Lab (www.shitanjia.com) for the TEM analysis.

Supplementary materials

Supplementary material associated with this article can be found, in the online version, at doi:10.1016/j.cclet.2022.03.110.

References

[1] R. Ungaro, S. Mehandru, P.B. Allen, et al., Lancet 389 (2017) 1756–1770.
[2] H. Hanai, T. Iida, K. Takeuchi, et al., Clin. Gastroenterol. Hepatol. 4 (2006) 1502–1506.
[3] J. Zhu, M. Xin, C. Xu, et al., Acta Pharm. Sin. B 11 (2021) 3193–3205.
[4] C. Zhang, Z. Chen, Y. He, et al., Chin. Med. 16 (2021) 92.
[5] C. Lahiff, A.C. Moss, Inflammatory Bowel Dis. 17 (2011) E66 -E66.
[6] C. Gao, C. Kwong, C. Sun, et al., ACS Appl. Mater. Interfaces 12 (2020) 25604–25615.
[7] T. Sun, C. Kwong, C. Gao, et al., Theranostics 10 (2020) 10106–10119.
[8] C. Gao, Q. Huang, C. Liu, et al., Nat. Commun. 11 (2020) 2622.
[9] Z. Chen, M.A. Farag, Z. Zhong, et al., Adv. Drug Delivery Rev. 176 (2021) 113870.
[10] H. Xu, R. Luo, L. Dong, et al., Nanomed.: Nanotechnol. Biol. Med. 39 (2021) 102461.
[11] M. Zu, Y. Ma, B. Cannup, et al., Adv. Drug Delivery Rev. 176 (2021) 113887.
[12] P. Liu, C. Gao, H. Chen, et al., Acta Pharm. Sin. B 11 (2021) 2798–2818.
[13] H. Lee, S.M. Dellatore, W.M. Miller, P.B. Messersmith, Science 318 (2007) 426–430.
[14] N.D. Catron, H. Lee, P.B. Messersmith, Biointerphases 1 (2006) 134–141.
[15] J. Xu, M. Tam, S. Samaei, et al., Acta Biomater 48 (2017) 247–257.
[16] X. Wang, H. Gu, H. Zhang, et al., ACS Appl. Mater. Interfaces 13 (2021) 33948–33961.
[17] H. Shi, X. Zhao, J. Gao, et al., Chin. Chem. Lett. 31 (2020) 3102–3106.
[18] S. Gou, Y. Huang, Y. Wan, et al., Biomaterials 212 (2019) 39–54.
[19] Z.G. Ma, R. Ma, X.L. Xiao, et al., Acta Biomater. 44 (2016) 323–331.
[20] L. Zhang, Y. Wang, X. Zhang, et al., ACS Appl. Mater. Interfaces 9 (2017) 3388–3399.
[21] G.P. Ramos, K.A. Papadakis, Mayo Clin. Proc. 94 (2019) 155–165.
[22] Y. Wu, J. Li, X. Zhong, et al., Asian J. Pharm. Sci. 17 (2022) 206–218.
[23] Y. He, Z. Chen, X. Nie, et al., Int. J. Biol. Macromol. 195 (2022) 102–116.
[24] Y.J. Shi, H.F. Gong, Q.Q. Zhao, et al., Toxicol. Lett. 315 (2019) 23–30.
[25] Y. Ding, T. Sun, S. Li, et al., ACS Appl. Biomater. 3 (2020) 10–19.
[26] Z. Guo, X. Cai, X. Guo, et al., Biochem. Pharmacol. 156 (2018) 196–203.
[27] P. Dejban, N. Nikravangolsefid, M. Chamanara, A. Dehpour, A. Rashidian, Phytother. Res. 35 (2021) 835–845.
[28] C. Li, G. Ai, Y. Wang, et al., Pharmacol. Res. 152 (2020) 104603.
[29] J. Xian, X. Zhong, H. Gu, et al., Pharmaceutics 13 (2021) 2005.
[30] S. Hasanzadeh, M.I. Read, A.R. Bland, et al., Phytother. Res. 159 (2020) 104921.
[31] S.J. Yue, W.X. Wang, J.G. Yu, et al., Phytother. Res. 148 (2019) 104453.
[32] M. Schirmer, A. Garner, H. Vlamakis, R.J. Xavier, Nat. Rev. Microbiol. 17 (2019) 497–511.
[33] N.R. Shin, T.W. Whon, J.W. Bae, Trends Biotechnol. 33 (2015) 496–503.
[34] Y. Wang, X. Gao, A. Ghozlane, et al., J. Crohn's Colitis 12 (2017) 337–346.
[35] Z.F. Dai, X.Y. Ma, R.L. Yang, et al., Exp. Ther. Med. 22 (2021) 1322.
[36] X. Song, L. Zhong, N. Lyu, et al., Genomics, Proteomics Bioinf. 17 (2019) 64–75.
[37] D. Piovani, S. Danese, L. Peyrin-Biroulet, et al., Gastroenterology 157 (2019) 647–659.e4.